JOURNAL OF MATERIALS SCIENCE 27 (1992) 3372–3378

Flexural strength of lapped and oxidized siliconized silicon carbide

W. J. TOMLINSON, S. KHELA
Department of Materials, Coventry Polytechnic, Coventry CV1 5FB, UK
C. A. JASPER, S. J. MATTHEWS
British Gas, Midlands Research Station, Solihull B91 2JW, UK

A siliconized silicon carbide composite has been microstructurally characterized, oxidized in air at 1350 °C for times up to 1079 h, air-cooled, and tested in four-point bending in the lapped condition at various temperatures up to 1425 °C, and in the pre-oxidized condition at room temperature and at 1300 °C. The strength of the lapped specimens increased by 25% at temperatures up to 1350 °C. Oxidation always decreased the strength of the material. After 315 h oxidation, the strength at room temperature and 1300 °C was reduced by 50% and 40%, respectively. Preferential oxidation of the inter-grain regions formed pits up to 50 μm deep. Hot salt corrosion increased the amount of oxidation by nearly 800%, and formed pits about 100 μm deep. Microstructural details of the oxidation and fracture processes are presented, and the possible mechanisms of failure discussed.

1. Introduction

Industrial gas-fired furnaces may lose the major part of the heat energy in the flue gases. Cross-flow heat exchangers can recover a substantial amount of the energy, and, for example, air preheat temperatures of about 1000 °C can theoretically save up to 70% of the fuel costs [1]. Heat exchangers must withstand intermittent heating to high temperatures and degradation by flue gases. They must also be manufactured with an intricate geometry of holes, in order to present a large exchange surface area and a minimum resistance to gas flow. Silicon carbide has, for a ceramic, an unusually high thermal conductivity which, with its good strength and high resistance to oxidation, make it a prime candidate for use in heat exchangers. Difficulties in fabricating large complex ceramic components may be reduced by infiltrating a shaped body of silicon carbide strips with silicon, and large heat exchanger blocks are manufactured from siliconized silicon carbide (SiSiC) composites [2].

Silicon and silicon carbide owe their high oxidation resistance to the formation of a protective film of silica. The formation, structure, and extent of protection, may vary considerably depending on the composition, type of material, and test conditions, and the overall position has been summarized by Frisch *et al.* [3]. Oxidation in air affects the strength of silicon carbide. Short periods of oxidation slightly increase the room-temperature strength by reducing the effect of surface flaws [4–8]. The effects of long periods of oxidation (up to 3500 h) under either static or cyclic conditions are complex [9–12], but generally the room-temperature strength is degraded by, at most, a few per cent. Deposits of small amounts of alkali compounds, notably Na_2SO_4, cause severe corrosion by forming a molten reaction product which dissolves the protective silica film and provides an increased transfer of oxygen to the silicon carbide surface [13, 14]. In contrast to the limited damage caused by oxidation in air, hot salt corrosion forms deep corrosion pits [8, 15–17] and may reduce the room-temperature strength by up to 40% [15].

There is only a small amount of information available on the oxidation and strength of siliconized silicon carbide [18, 19]. The room-temperature strength increased from 312 MPa to 405 MPa after oxidation at 1370 °C for 2160 h [18]. The strengthening was considered to be due to internal nitridation. The strength decreased in dry hydrogen–nitrogen atmospheres, and was relatively unaffected by thermal cycling [18]. Butt *et al.* [19] using a combustion facility, showed that oxidation at 900–1050 °C in a high-velocity air–natural gas mixture containing sodium silicate, reduced the strength of SiSiC by approximately 50%. Thus the oxidation and strength of SiSiC may vary considerably depending on the test conditions, and with the use of SiSiC in heat exchangers in mind, the present work investigated the strength of lapped SiSiC at temperatures up to 1425 °C, and the effects of pre-oxidation for times up to 1079 h at 1350 °C on the strength at room temperature and at 1300 °C.

2. Experimental procedure

A single batch of SiSiC plates normally used in the construction of heat exchangers was used. Full manufacturing details are not available, but typically

0022–2461

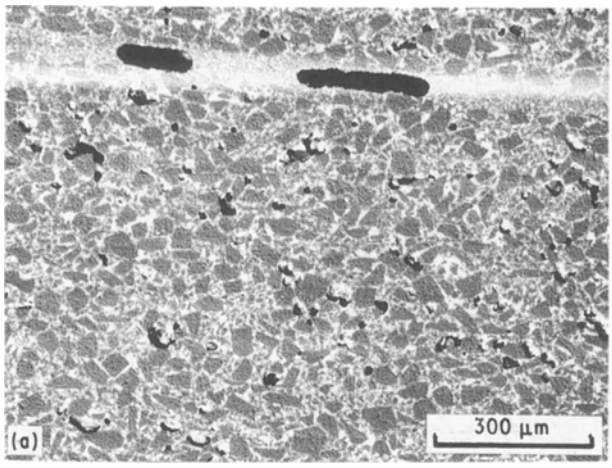

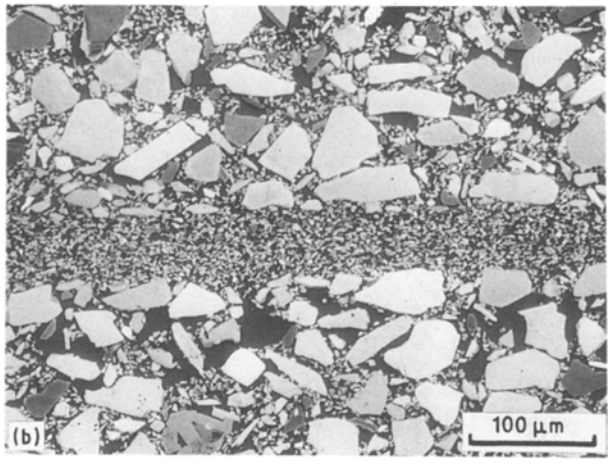

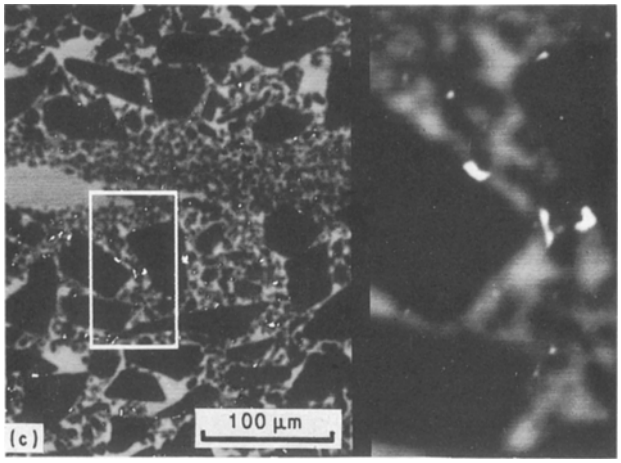

Figure 1 Cross-section of the SiSiC material. (a, b) Tape regions and bonding layer: (a) note elongated porosity in bonding layer; (b) note porosity in tape regions. (c) Back-scattered image showing bright spots (iron) next to SiC surface. SEM. Unetched.

flexible tapes containing 50%–70% SiC powder with various additives are laminated to produce the required shape, heat treated to consolidate the green body, and infiltrated with silicon [2]. The present material consisted of tape-cast layers 0.8 mm thick, bonded by infiltrated silicon layers about 50 μm thick (Fig. 1). The SiC grains were typically about 40 μm in size, with the largest about 50 μm. Judging from the amounts of calcium and aluminium in the oxidized layer (see later), the silicon-rich matrix contained small amounts of calcium and aluminium. Small amounts of iron and potassium were also present. The iron was located at the SiC surface (Fig. 1c), but the other elements were dispersed. The infiltrated silicon contained a mass of grains 2–5 μm in size.

Image analysis at about 20 random positions in the tape regions of a polished section showed porosities of about 3–5%. Similar values were measured on a number of other sections. Microscopical details of the porosity are shown in Fig. 1a and b, and also in Fig. 6 (see later). In a number of cases, infiltration of silicon was not complete (Fig. 1a), and sometimes up to about 20% porosity occurred (Fig. 6b). This may be compared with Fig. 6a which shows virtually no porosity in the silicon regions.

Flexure bars 3 × 3 × 56 mm were cut parallel to the tape surface (see Fig. 6a and b), diamond lapped to 14 μm, and ultrasonically cleaned in acetone. The roughness of nine faces in the lapped condition over a 2 mm length was measured using a microcomputer-controlled Talysurf, and the parameters R_a (centreline average), R_t (vertical height from highest peak to lowest trough), skewness Sk and kurtosis Ku, calculated. Skewness and kurtosis characterize the shape of the profile, and an ideal Gaussian roughness has $Sk = 0$ and $Ku = 3$ [20, 21]. Two surfaces had a roughness that was approximately Gaussian with $R_a = 0.07$ μm and $R_t = 0.7$–0.8 μm. Traces on the other seven faces showed the distinct presence of a few deep holes, and now the roughness values were in the ranges R_a 0.10–0.59 μm and R_t 3.8–6.9 μm.

Specimens were tested in four-point bending on the tape region face (see Fig. 6a and b), with an inner and outer separation of 19.6 mm and 39.6 mm, respectively, using an Instron 4204 with a crosshead speed of 0.5 mm min^{-1}. Testing in air at elevated temperatures followed the procedure: ramp the specimen at 10 °C min^{-1} to the test temperature (typically 1300 °C), hold for 15 min, test to failure, and then cool naturally in the instrument over a period of about 2 h. Specimens were tested in the lapped and in the pre-oxidized conditions.

Oxidation consisted of supporting the specimens on SiSiC bars on an SiSiC tray, inserting the tray with specimens into an electric muffle furnace stabilized at 1300 °C, oxidizing in air, and then removing the tray from the furnace to cool in air. Oxidized specimens were always air-quenched to room temperature in this manner, irrespective of the temperature at which they were later tested. Hot salt corrosion was also briefly investigated. For this, a film of Na_2SO_4 (nominally 2 mg cm^{-2}) was deposited by spraying a saturated solution of Na_2SO_4 on to the hot specimen (about 200 °C) before oxidation [13–16].

3. Results and discussion

Specimens failed in bending with very little prior deformation, and the mean fracture stress for all the tests are collected in Tables I and II. The mean fracture stress of the lapped specimens increased by nearly 25% at 900–1300 °C (Table I). At the highest

TABLE I Strength of lapped specimens at various temperatures

Test temperature (°C)	Number of specimens	Modulus of rupture			Weibull modulus
		Mean (MPa)	S.D. (MPa)	Coefficient of variation, 100 (S.D./mean) (%)	
20	24	263	48	18	4
900	5	310	13	4	25
1000	3	326	15	5	18
1100	5	302	21	7	14
1200	5	324	11	3	28
1300	5	318	23	7	13
1350[a]	2	–	–	–	–
1425	1	18	–	–	–

[a] Samples did not break.

TABLE II Strength of specimens oxidized in air at 1350 °C for various times, cooled, and tested either at 20 °C or reheated and tested at 1300 °C

Testing temperature (°C)	Oxidation time (h)	Number of specimens	Modulus of rupture			Weibull modulus
			Mean (MPa)	S.D. (MPa)	Coefficient of variation, 100 (S.D./mean) (%)	
20	0	24	263	48	18	4
	50	10	176	26	15	5
	100	10	182	14	8	21
	315	10	149	26	17	5
	503	10	141	20	14	7
	1079	10	177	17	10	20
1300	0	5	318	25	8	22
	50	10	292	25	9	12
	100	2	218	4	–	42
	315	2	199	12	–	15
	503	4	231	24	10	4
	1079	5	225	30	13	7

temperatures (1350 and 1425 °C) extensive plastic deformation occurred and sometimes the specimen did not break. Pre-oxidation at 1350 °C always substantially decreased the strength of the specimens. The decreases in strength occurred progressively with oxidation time, being most rapid after only small periods of oxidation and then staying much the same for oxidation times of 315–1079 h (Fig. 2). With respect to the lapped condition at the same temperature of testing, after 315 h pre-oxidation, the decrease in strength at room temperature and at 1300 °C was $(318 - 149)/318 = 0.53$ and $(318 - 199)/318 = 0.37$ times, respectively. With respect to the strength at room temperature, a maximum decrease by $(263 - 141)/263 = 0.46$ times occurred after pre-oxidation for 503 h.

Although the number of specimens tested is limited in some cases, two points are made concerning the distribution in strength. First, oxidation increases the scatter. Second, except for one isolated point, results from all the 130 tests were, for each test condition, closely associated with a single Weibull line (not illustrated), with no indication of a break or change of slope.

Details of the oxidation reaction products formed after various times at 1350 °C are given in Figs 3–5 and in Table III. The thickness of the oxide layer on the surface was relatively uniform (Fig. 3), and the

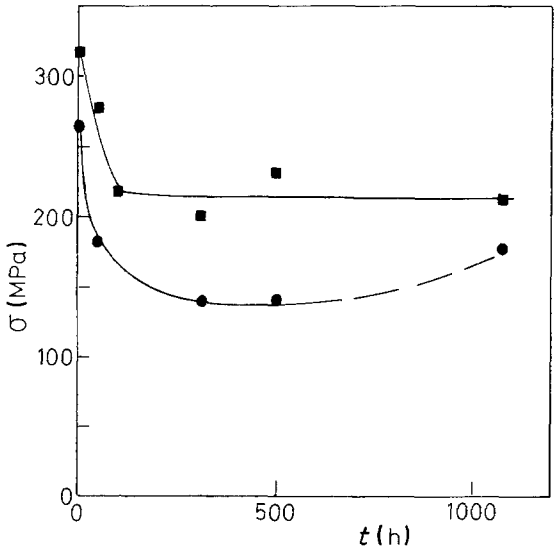

Figure 2 Average fracture stress, σ, as a function of pre-oxidation time, *t*, at 1350 °C in air. Tested at (●) room temperature, and (■) 1300 °C.

measured oxide thicknesses followed closely a parabolic oxidation law $y^2 = kt$, with parabolic rate constant $k = 6.5 \times 10^{-17}$ m^2 s^{-1}, over the entire exposure period (Fig. 4). An important feature of the oxidation process is the preferential oxidation of the matrix which produces an irregular and deeply pitted substrate/reaction product interface (Fig. 3). It is seen that

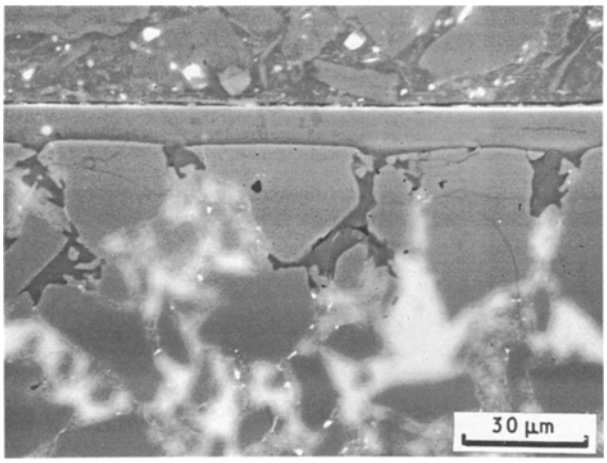

Figure 3 Section of the material oxidized for 503 h in air at 1350 °C and then air cooled, showing uniform surface oxide layer and deep inter-grain oxidation.

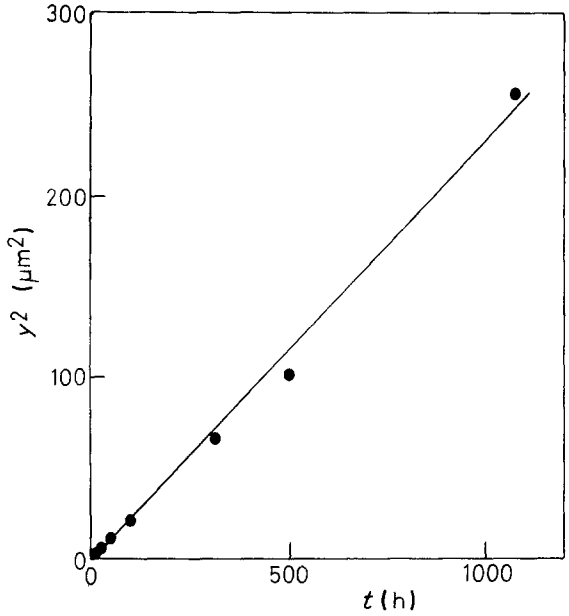

Figure 4 Surface layer thickness, y, as a parabolic function of the oxidation time, t, in air at 1350 °C.

the intergrain oxidation does not have a simple geometry, because it is determined by the adventitious morphology of the adjacent SiC grains. Analysis of the oxide by EDX and element mapping showed, in addition to the presence of silicon, significant amounts of calcium and aluminium.

Cracking occurred in specimens cooled in air from the temperature of oxidation. In the oxidized layer, cracking was observed on the surface after oxidation times up to 315 h (Fig. 5a and Table III). The two large, crack-free, light-shaded areas are regions of amorphous silica. Although not evident on the surface, specimens oxidized for longer times were cracked near the substrate surface, and particularly within the pits formed by preferential oxidation of the matrix (Fig. 5b; see also Fig. 7b). Occasionally, severe cracking of the SiSiC occurred near the surface after short periods of oxidation (Fig. 5c). Such severe damage did not occur after extended periods of oxidation (cf. Figs 3 and 7).

A number of fracture faces were examined (Fig. 6). In most cases it was difficult to locate the initiation site, or, when located, to establish the nature of the initiation flaw. However, due to the specimen and testing geometry whereby only the tape regions were at the surface, it is clear that the massive inter-tape porosity was never associated with fracture initiation, although it did influence the subsequent crack path (Fig. 6b).

Brittle ceramics typically fail due to the presence of a surface flaw. The fracture strength, σ, is determined

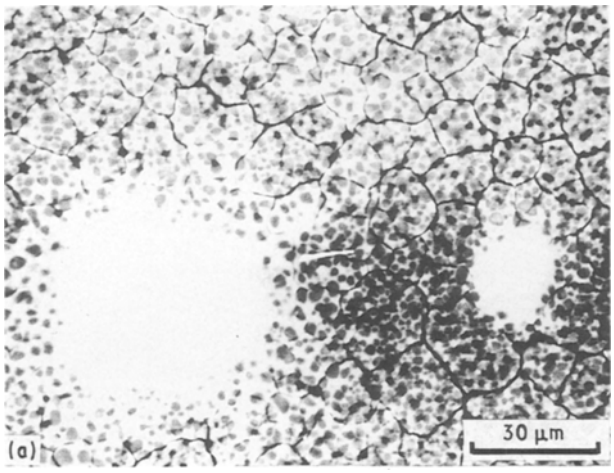

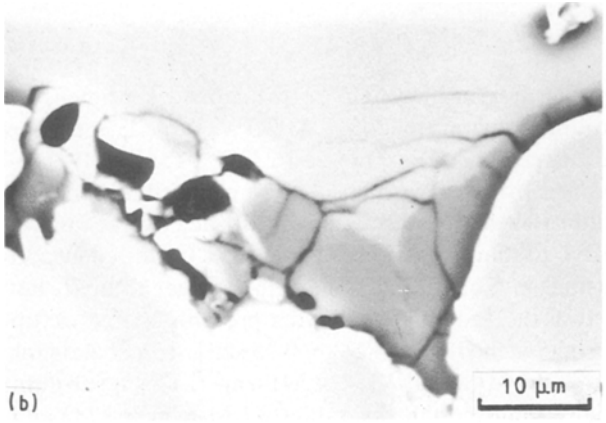

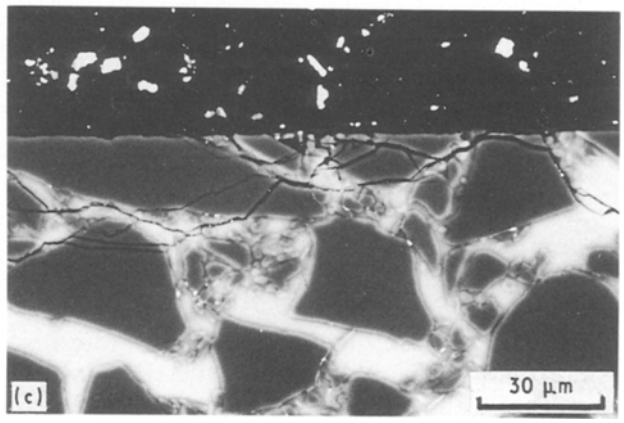

Figure 5 (a) Plan showing the surface cracking in the glass formed on a specimen oxidized for 50 h. (b) Section showing the cracked oxide within a pit formed on a specimen oxidized for 1079 h. (c) Section showing extensive cracking in the surface regions of SiSiC on a specimen oxidized for 5 h. SEM. Unetched.

TABLE III Oxide characteristics on specimens oxidized in air at 1350 °C for various times

Oxidation time (h)	Oxide thickness [a]			Maximum depth of penetration[b] (μm)	Oxide cracking[c]	Sound on cooling[d]
	Mean (μm)	S.D. (μm)	Coeff. of variation, 100 (S.D./mean) (%)			
5	1.0	–	–	–	Yes	Yes
24	2.3	0.48	43	–	Yes	Yes
50	3.3	0.95	29	–	Yes	Yes
100	4.6	0.88	19	9	Yes	Yes
315	8.1	1.54	19	15	Yes	Yes
503	10.1	1.48	15	41	No	Yes
1079	16.0	0.97	6	48	No	No

[a] See Fig. 3. Mean of 20 measurements over approximately 3 mm, except for 5 h sample where layer was too thin to measure in some areas.
[b] Approximate maximum depth of oxidation in the silicon observed in one section; see Fig. 3, and text.
[c] As seen on surface. See Fig. 5 and text.
[d] Audible sound after removal from hot furnace. See text.

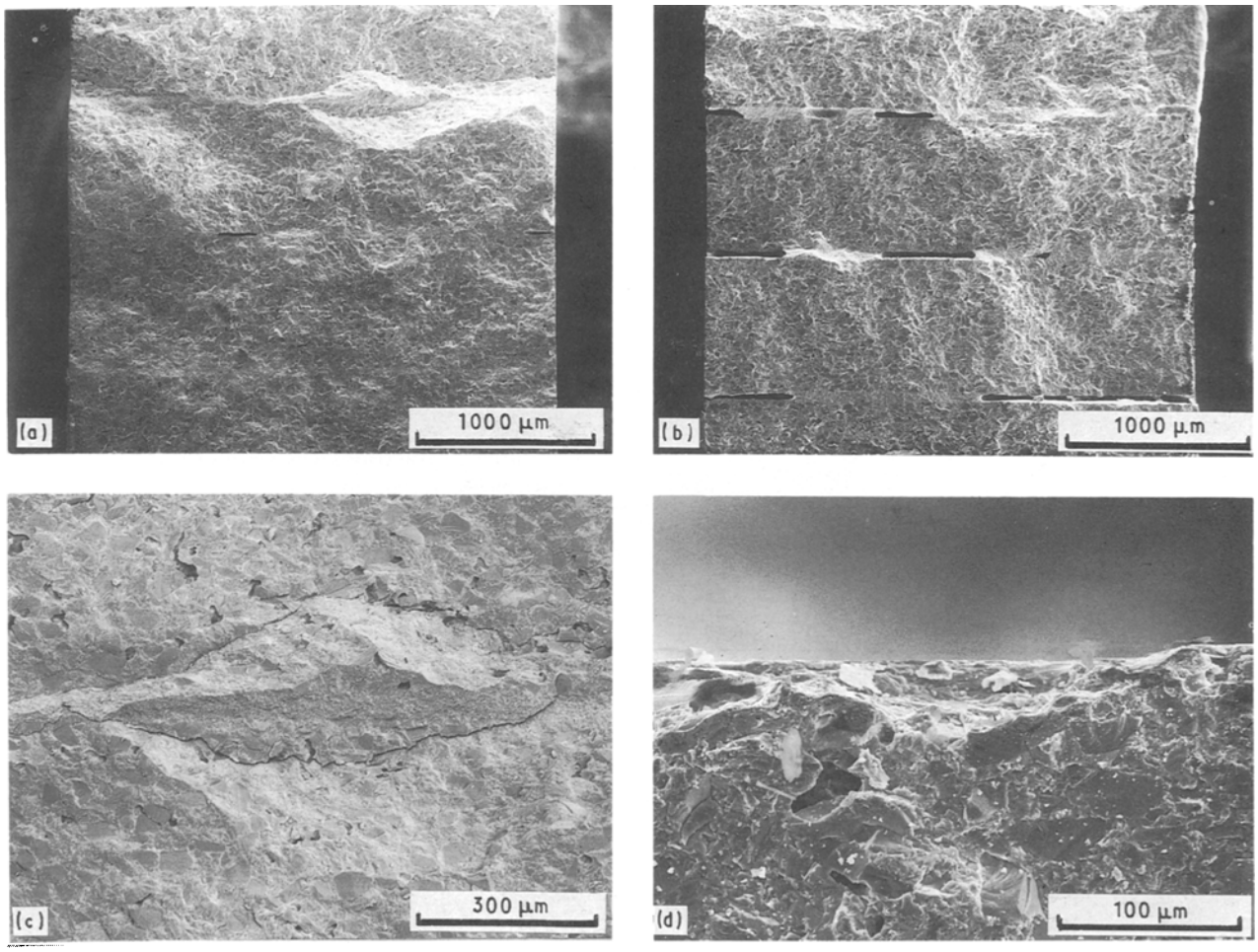

Figure 6 Fracture faces of specimens tested at room temperature showing (a) material with virtually no inter-tape porosity, (b) considerable inter-tape porosity, (c) general porosity in the tape region, and (d) a possible initiation site. (a–c) as lapped, (d) oxidized for 50 h.

by a geometrical flaw of depth c at the surface according to the Griffith relation

$$\sigma_f = (Y/Z)\,(K_{Ic}/c^{1/2}) \quad (1)$$

where Y and Z are geometrical constants and K_{Ic} is the fracture toughness [22]. Frequently Y/Z is taken to be about 0.75 [23]. Grinding damage and residual stresses may also contribute to the fracture process or control it [24–26], and in some cases the strength may be reduced by up to 50% [26].

The fracture strength of the lapped specimens at room temperature, 263 ± 48 MPa (Table I) is similar to values 312 MPa [18] and 239 ± 34 MPa [19] obtained by other workers. The single Weibull function indicates that the strength is controlled by one kind of flaw. Assuming the porosity acts as a Griffith flaw and using, in Equation 1, $c = 10$ μm (larger than R_t because the radius of the stylus prevents the crack tip being reached) and $(Y/Z) = 0.75$ [23], we calculate for $\sigma = 263$ MPa that $K_{Ic} \approx 1$ MPa $m^{1/2}$. This is substantially smaller than the values 3.1 MPa $m^{1/2}$ [23] and

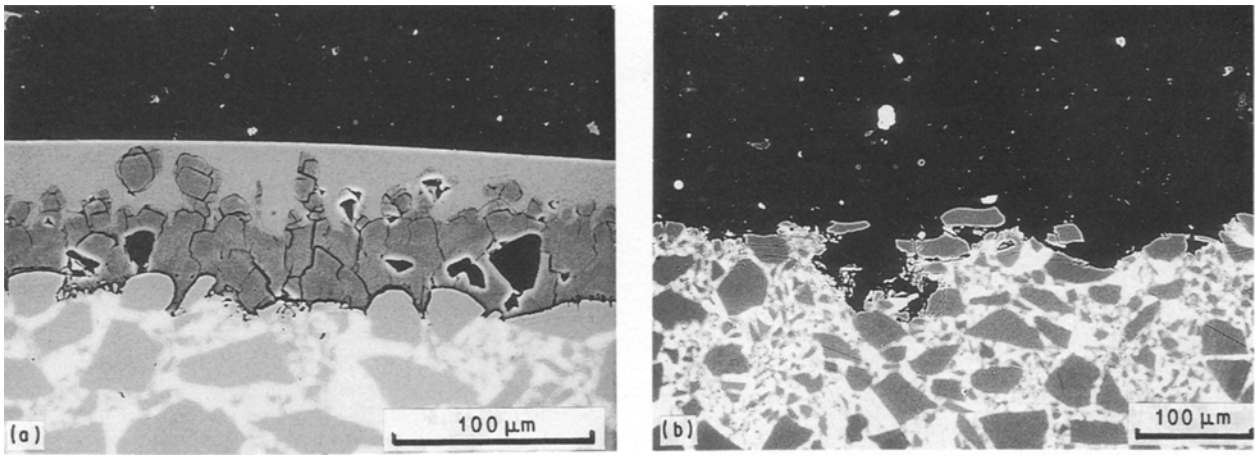

Figure 7 Sections of specimens hot-salt corroded for 503 h at 1350 °C. (a) Sections showing reaction products and (b) section after removal of the reaction products. Note the large pit in (b) formed by preferential oxidation of the matrix surrounding an SiC grain leading to its removal on dissolving the reaction products in hot HF solution. SEM. Unetched.

3.4 MPa $m^{1/2}$ [27] measured on sintered silicon carbide, which suggests that other factors are also influencing the fracture process. In the present case, it is suggested that grinding damage is the main factor effectively reducing the strength of the material [8].

Degradation in strength after oxidation is considered to be due primarily to the formation of deep inter-grain oxidation (Fig. 3 and Table III) which act effectively as surface cracks. For example, again assuming an original crack length of 10 μm, inter-grain oxidation to a depth of 41 μm (after 503 h, Table III), will reduce the strength to 263 $(10/41)^{1/2}$ = 130 MPa; i.e. by about 50%. This is very approximate, but it is of the right order and illustrates the process. However, two other factors are important, and help determine the shape of the fracture stress–oxidation time curve (Fig. 2).

First, after short periods of oxidation, air-quenching produces a substantial amount of thermal stress and cracking (Fig. 5c) which will clearly promote fracture. It is suggested that this is only effective in combination with the residual grinding damage. On this basis, thermal stresses due to air-quenching the specimens will only be fully effective after short periods of oxidation, because prolonged oxidation at 1350 °C will reduce the severity of the grinding damage by annealing, and also progressively eliminate the damaged layers by conversion to oxidation products.

Second, after extended periods of oxidation, the morphology of inter-grain oxidation changes. Once the depth of penetration is similar to the size of a typical SiC grain (about 40 μm), the oxidation front spreads out to oxidize the matrix behind the SiC particle. But at the same time, the inward supply of oxygen to the reaction front is limited and fixed by the minimum gap between adjacent SiC particles. These two factors combine to slow down the rate of penetration and reduces the effectiveness of the inter-grain oxidation to act as a crack in the Griffiths sense (Equation 1). These changes are reflected in the shape of the strength–oxidation time curve (Fig. 2).

Microscopical results from limited hot salt corrosion tests are shown in Fig. 7. After 503 h at 1350 °C, the reaction products formed a layer about 70 μm thick, consisting of an outer region of glass and an inner region of crystalline silica. Removal of the oxides with hot HF solution [13, 14] showed clearly the preferential attack of the silicon matrix and the formation of pits about 100 μm deep (Fig. 7b). Compared with oxidation in air (Table III), the presence of Na_2SO_4 increased the amount of oxidation by (70 − 8)/8 = 7.75 times, i.e. by nearly 800% and increased the pit size by (100 − 40)/40 = 1.5 times, i.e. by 150%. No strength measurements were made, but again assuming the prime importance of the roughened and pitted surface in determining the fracture strength, we estimate pits of the order 100 μm to reduce the strength by $(10/100)^{1/2}$ = 0.3 times. This is very approximate, but it illustrates the extent of the damage that can occur.

Finally, we comment on the massive porosity in the infiltrated regions. Owing to the orientation of the specimens machined from plates of material and the method of testing, only the tape surfaces were directly involved in oxidation and initiation of fracture. It is important that the transverse oxidation and strength properties of the material are determined, because the silicon-infiltrated regions can produce notches that may greatly reduce the strength in two ways: by rapid and deep preferential oxidation of the silicon, or by occasional incomplete filling with silicon during manufacture.

4. Conclusions

1. The siliconized silicon carbide composite (SiSiC) consisted of layers of tape-cast regions 0.8 mm thick joined by infiltrated silicon regions about 50 μm thick. The tape regions contained SiC grains typically about 40 μm in size, in a matrix of silicon containing significant amounts of calcium and aluminium. It had about 4% porosity. The silicon bonding layer frequently had a massive porosity due to incomplete infiltration.

2. Lapped specimens had typical roughness, R_a = 0.10–0.59 μm, and R_t = 3.8–6.9 μm. In all tests, the surface exposed consisted of the tape regions.

3. The strength of the lapped specimens at room temperature was 263 MPa. The strength was increased by 25% at temperatures up to 1350 °C.

4. Specimens oxidized in air at 1350 °C for times up to 1079 h and then air-quenched were tested at room temperature and at 1300 °C. After 315 h oxidation, the strength at room temperature and at 1300 °C compared with the lapped condition, was reduced by 50% and 40%, respectively. Longer periods of oxidation had relatively little effect on the strength.

5. Oxidation at 1350 °C resulted in an oxide layer that formed according to a parabolic oxidation law, and preferential inter-grain oxidation that roughened the surface and formed deep pits. Extensive cracking of the oxides and surface material was associated with air-quenching.

6. Hot salt corrosion increased the oxidation rate by nearly 800%, and formed pits about 100 μm in the material.

7. It is suggested that the primary mechanism of failure of the oxidized specimens is by the preferentially oxidized matrix regions acting as stress-concentrating flaws. The effects of grinding damage, thermal stresses generated by air-quenching, and prolonged oxidation at high temperature, are also considered and related to the fracture processes. There was no evidence that the occasional presence of massive porosity in the siliconized layers significantly influenced the results.

Acknowledgements

The authors thank A. J. Jinkels, British Gas Research, Solihull, for encouragement and the provision of facilities, and P. Brennen, Coventry Polytechnic, for help with the roughness measurements.

References

1. M. COOMBS, H. STRUMPF and D. KOTCHICK, in "International Gas Research Conference", Chicago, IL, June 1983.
2. J. HEINRICH, J. HOOVER, J. HUBER, S. FORSTER and T. QUELL, *Indust. Ceram.* 7 (1987) 34.
3. B. FRISCH, W. R. THIELE, R. DRUMM and B. MUNNICH, *Ber. DKG* **65** (1988) 277.
4. D. E. SCHWAB and M. M. KOTCHICK, *Amer. Ceram. Soc. Bull.* **59** (1980) 805.
5. F. F. LANGE, *J. Amer. Ceram. Soc.* **53** (1970) 290.
6. T. E. EASLER, R. C. BRADT and R. E. TRESSLER, *ibid.* **64** (1981) 731.
7. W. J. TOMLINSON and D. M. CASLIN, *Ceram. Int.* **17** (1991) 61.
8. W. J. TOMLINSON and J. FARRELL, *ibid.*, in press.
9. Y. TAKEDA and K. NAKAMURA, in "Proceedings of the Annual Meeting of the Ceramic Society of Japan", Okayama, 22-24 May 1985, pp. 459–60.
10. W. D. CARRUTHERS, in Proceedings of the Automotive Technology and Development Contractor Coordination Meeting, Michigan, 26-29 October 1981, pp. 427–43.
11. M. MAEDA, K. NAKAMURA, T. OHKUBO and T. ISHIGUKA, *Ceram. Int.* **15** (1989) 1.
12. M. MAEDA, K. NAKAMURA and M. YAMADA, *J. Amer. Ceram. Soc.* **72** (1989) 512.
13. N. S. JACOBSON and J. L. SMIALEK, *ibid.* **68** (1985) 432.
14. N. S. JACOBSON, *ibid.* **69** (1986) 74.
15. N. S. JACOBSON, C. A. STEARNS and J. L. SMIALEK, *Adv. Ceram. Mater.* **1** (1986) 154.
16 J. L. SMIALEK and N. S. JACOBSON, *J. Amer. Ceram. Soc.* **69** (1986) 741.
17. N. S. JACOBSON and J. L. SMIALEK, *J. Electrochem. Soc.* **133** (1986) 2615.
18. R. FORTHMANN and A. NAOUMIDIS, *Mater. Sci. Engng* **A121** (1989) 457.
19. D. P. BUTT, J. J. MECHOLSKY and V. GOLDFARB, *J. Amer. Ceram. Soc.* **72** (1989) 1628.
20. K. J. STOUT, *Mater. Engng* **2** (1981) 260.
21. *Idem., ibid.* **2** (1981) 287.
22. D. W. RICHERSON, "Modern Ceramic Engineering" (Marcel Dekker, New York, 1982).
23. M. A. JANNEY, *Amer. Ceram. Soc. Bull.* **66** (1987) 322.
24. G. WILLMANN, *Ceram. Indust. J.* December (1985) 15.
25. M. HAKULINEN, *J. Mater. Sci.* **20** (1985) 1049.
26. C. C. WU and K. R. McKINNEY, in "The Science of Ceramic and Surface Finishing II", edited by B. J. Hockey and R. W. Rice (National Bureau of Standards SP562, Washington, DC, 1979) p. 477.
27. W. J. TOMLINSON and J. C. WHITNEY, *Ceram. Int.*, in press.

Received 13 September
and accepted 26 September 1991